DOI: 10.1111/exd.12296
www.wileyonlinelibrary.com/journal/EXD

Original Article

Molecular interactions of plant oil components with stratum corneum lipids correlate with clinical measures of skin barrier function

Mary Catherine Mack Correa[1], Guangru Mao[1], Peter Saad[2], Carol R. Flach[2], Richard Mendelsohn[2] and Russel M. Walters[1]

[1]Johnson & Johnson Consumer Companies, Inc., Newark, NJ, USA; [2]Department of Chemistry, Rutgers University, Newark, NJ, USA
Correspondence: M. C. Mack Correa, Johnson & Johnson Consumer Companies, Inc.,199 Grandview Road Skillman, Newark, NJ 08558, USA, Tel.: +1 908 874 1373, Fax: +1 908 874 2615, e-mail: ccorrea1@its.jnj.com

Abstract: Plant-derived oils consisting of triglycerides and small amounts of free fatty acids (FFAs) are commonly used in skincare regimens. FFAs are known to disrupt skin barrier function. The objective of this study was to mechanistically study the effects of FFAs, triglycerides and their mixtures on skin barrier function. The effects of oleic acid (OA), glyceryl trioleate (GT) and OA/GT mixtures on skin barrier were assessed *in vivo* through measurement of transepidermal water loss (TEWL) and fluorescein dye penetration before and after a single application. OA's effects on stratum corneum (SC) lipid order *in vivo* were measured with infrared spectroscopy through application of perdeuterated OA (OA-d_{34}). Studies of the interaction of OA and GT with skin lipids included imaging the distribution of OA-d_{34} and GT *ex vivo* with IR microspectroscopy and thermodynamic analysis of mixtures in aqueous monolayers. The oil mixtures increased both TEWL and fluorescein penetration 24 h after a single application in an OA dose-dependent manner, with the highest increase from treatment with pure OA. OA-d_{34} penetrated into skin and disordered SC lipids. Furthermore, the *ex vivo* IR imaging studies showed that OA-d_{34} permeated to the dermal/epidermal junction while GT remained in the SC. The monolayer experiments showed preferential interspecies interactions between OA and SC lipids, while the mixing between GT and SC lipids was not thermodynamically preferred. The FFA component of plant oils may disrupt skin barrier function. The affinity between plant oil components and SC lipids likely determines the extent of their penetration and clinically measurable effects on skin barrier functions.

Key words: oleic acid – skin barrier – skin lipids – stratum corneum

Accepted for publication 29 November 2013

Introduction

The quality of skin barrier function is primarily determined by the structural order of intercellular stratum corneum (SC) lipids, the only continuous transport route throughout SC (1). SC lipids, comprised of ceramides, cholesterol and free fatty acids (FFAs), form ordered structures in multiple dimensions. The lipids arrange in lamellar layers with repeat distances of 6 and 13 nm (2). Laterally, SC lipids organize in orthorhombic and hexagonal crystalline phases (3) with some disordered lipids also present (4). Perturbation of the lamellar organization increases drug permeability in SC lipid models (5). Prevalence of the more tightly packed orthorhombic phase has been shown to correlate with higher SC integrity and barrier efficiency as measured by transepidermal water loss (TEWL) (4,6).

The structural organization of SC lipids is affected by both pathological conditions and the permeation of exogenous materials. *In vitro* models have also demonstrated that SC lipid composition affects structural order and water transport properties, thus presenting opportunities for development of therapeutic interventions to normalize lipid composition, restoring barrier function (7–9). Abnormal lamellar structure and disrupted lateral order have been associated with compromised barrier function clinically in patients with psoriasis, ichthyosis and atopic dermatitis as well as preclinically in cultured models of the epidermis (1,10–15). Additionally, exogenous compounds from topical skincare products can affect SC lipid molecular order. Surfactants are well known to perturb the skin barrier through endogenous lipid removal and disordering (16–18). The penetration of actives and delivery systems has been shown to disrupt SC lipid structural order (19–21) and is often associated with increased TEWL (22).

The effects of the permeation enhancer, oleic acid (OA), on skin barrier function have been widely studied. *In vivo*, OA caused a significant increase in TEWL and skin irritation (23). Similar TEWL increases were also observed in mouse models, and OA was suggested to alter the calcium dynamics in epidermal keratinocytes (24). OA was found to predominantly interact with SC lipids rather than keratin (25,26). Two mechanisms have been proposed to understand OA's interaction with SC lipids: disordering of SC lipids and formation of separate disordered OA enriched domains (27,28). More recent studies showed that OA promoted phase separation in SC lipids (29) while molecular dynamic simulations suggested that OA reduced SC lipid bilayer density and thickness (30). Furthermore, aqueous monolayer studies from our laboratory demonstrated that interactions between OA and an SC lipid model depended on composition and the physicochemical status of SC lipids, with either of the previously proposed mechanisms dominating under different conditions (31).

Plant-derived oils are becoming more prevalent in skincare product formulations. The chemical compositions of these oils consist primarily of triglycerides with various fatty acid chains and small fractions of FFAs (32,33). Commonly, oil-based formulations form an occlusive layer on the skin surface with penetration

no further than the first few layers of the SC (34). However, hydrolysing conditions during manufacturing and storage may elevate FFA content in products. In addition, FFAs can be added directly to products as emollients or emulsifying agents. FFAs are known to penetrate into SC and enhance the permeation of other species (35,36). In this study, mixtures of OA and glyceryl trioleate (GT) were used to mimic the natural oils used in skincare formulations to better understand their effects on skin barrier function. *In vitro*, *ex vivo* and *in vivo* experiments were performed using Langmuir monolayer, infrared spectroscopy, TEWL and fluorescent dye penetration techniques.

Methods

Materials

Bovine brain ceramide (type III), cholesterol, palmitic acid, oleic acid (99%), glyceryl trioleate (99%), deuterated oleic acid (OA-d_{34}, 98 atom% D), chloroform (99%), 1-octanol (99.5%), sodium chloride (99%) and EDTA tetrasodium salt (99%) were purchased from Sigma-Aldrich (St. Louis, MO, USA). The ceramide belongs to the NS ceramide family with non-hydroxy fatty acid chains composed predominantly of stearic acid (C18:0) and nervonic acid (C24:1) attached to a sphingosine headgroup through an amide bond. D&C Yellow #8 (fluorescein) was purchased from Sensient Cosmetic Technologies (South Plainfield, NJ, USA). All chemicals were used without further purification.

Clinical protocol

Caucasian female subjects, Fitzpatrick skin types I–III, aged 21–40 years were recruited to participate in two studies. The subjects were in general good health with no history of skin disease and had no lesions or marks on the volar forearms which would interfere with the study measurements. The study protocols were approved by the Allendale Investigational Review Board (Old Lyme, CT, USA) and conducted in accordance with the ethical principles of the declaration of Helsinki. Written informed consent was obtained from all participants prior to enrolment.

Twelve subjects participated in Study 1. Five 2×6 cm^2 areas were marked on volar forearms, and baseline measurements were acquired after 30-min acclimatization to room conditions. Four sites were treated with oils according to a randomization scheme, leaving one site as an untreated control. For the treated sites, 48 μl of either 100% OA, 50% OA/50% GT, 25% OA/75% GT or 100% GT (wt%) was gently rubbed onto the skin with a presaturated gloved finger. All sites were then covered with gauze. Plastic wraps were supplied to cover the arms while bathing. Measurements were taken 24 h after the treatment following 30-min room acclimatization.

Two subjects were included in Study 2. Two 2×6 cm^2 sites were marked on volar forearms with one site treated with OA-d_{34} and the other serving as an untreated control. Treatments and measurements followed the same procedure as in Study 1, with the addition of an attenuated total reflectance–Fourier transform infrared spectroscopy (ATR-FTIR) measurement.

Clinical evaluations

TEWL was measured with a Vapometer (Delfin Technologies, Kuopio, Finland). Penetration of fluorescein was measured after 24 h on a subset of subjects ($n = 5$) in Study 1. Fluorescein (0.15% in water) was patched on each site for 1 h, and fluorescence confocal image stacks were collected with the Vivascope 1500 (Lucid Technologies, Rochester, NY, USA) using 445 nm laser illumination. Three image stacks were collected on each treatment site. Fluorescein penetration was assessed semi-quantitatively through fluorescence intensity profiles. Two or three regions of interest (ROI's) were selected in each fluorescence image stack, taking care that the ROIs did not overlap with epidermal glyphics. The mean intensity, normalized by illumination laser power, was calculated as a function of depth for each ROI using Matlab (The Mathworks, Nantick, MA, USA). Average fluorescence intensity depth profiles for each treatment were calculated by first averaging the intensity at each depth in all ROI's per site and then averaging the site intensity depth profiles from all subjects. ATR-FTIR spectra were taken with a Thermo Nicolet Nexus 670 FTIR Spectrometer, equipped with 2×0.2 inch ZnSe ATR crystal (Thermo Scientific, Waltham, MA, USA) in Study 2. Two duplicate spectra were collected and averaged at each site with 128 scans and 4/cm spectral resolution.

Ex vivo sample preparation

Human surgical abdominal skin (otherwise to be discarded) was obtained with informed consent and ethics board approval. Skin samples were tape-stripped twice to remove surface sebum and attached to home-built diffusion cells with the SC facing the donor chamber (8 mm in diameter). ~120 μl of OA-d_{34} or GT was added to the donor chamber while the receptor was left empty. Samples were incubated at 34°C for 24 h. Excess liquid was removed after incubation, and the skin surface was cleaned with cotton swabs. Skin sections, ~8 μm thick, were microtomed perpendicular to the skin surface for IR imaging.

Ex Vivo IR microspectroscopic imaging

IR microspectroscopic images of skin cross-sections were collected with a PerkinElmer Spotlight 300 system (PerkinElmer Life and Analytical Sciences, Inc., Waltham, MA, USA). The procedure was described in detail previously (37). Thirty-two spectra with a spectral resolution of 4/cm were averaged for each 6.25×6.25 μm pixel. Visible images of the sampled skin regions were acquired with the integrated microscope. Absolute concentrations of OA-d_{34} and GT were calculated with extinction coefficients determined from their respective octanolic solutions.

Monolayer measurements

A KSV NIMA Langmuir trough (KN1006, Biolin Scientific, Stockholm, Sweden) was used to acquire surface pressure-molecular area (π-A) isotherms. Monolayers were floated on a subphase of 150 mM NaCl and 1 mM EDTA adjusted to pH 5.5. Typically, ~60–80 μl of ~1 mg/ml lipid/chloroform solution was spread at air–water interface, and 15 min were allowed for solvent evaporation. Monolayers were then compressed with a constant barrier speed of ~4 Å^2/molecule/min until collapse. The miscibility between monolayer components was quantified using the surface excess Gibbs energy of mixing, ΔG_{ex} (Eqn 1).

$$\Delta G_{ex} = N \int_0^{\pi} [A_{12} - (X_1 A_1 + X_2 A_2)] d\pi \quad (1)$$

where N is Avogadro's constant, A_{12}, A_1 and A_2 are the mean molecular areas for the mixed monolayers, and monolayers of components 1 and 2, while X_1 and X_2 are the mole fractions of each component in the mixture.

Results

Clinical measures of barrier function

Epidermal barrier function was assessed *in vivo* through TEWL measurements before and after topical treatments (Fig. 1a–b). Compared with the baseline TEWL value, no statistically significant change was detected after 24 h in both the untreated sites and sites treated with 100% GT. However, TEWL at sites treated with OA or OA/GT mixtures increased significantly from the baseline level. TEWL increases monotonically at sites treated with higher OA content (Fig. 1a), indicating that OA disrupts the skin barrier and facilitates water transport. The change in TEWL after treatment with OA and 50%OA/50%GT was also found to be significantly higher than 25% OA/75% GT, 100% GT and untreated control. Within-subject changes in TEWL follow the same trend observed in mean values (Fig. 1b).

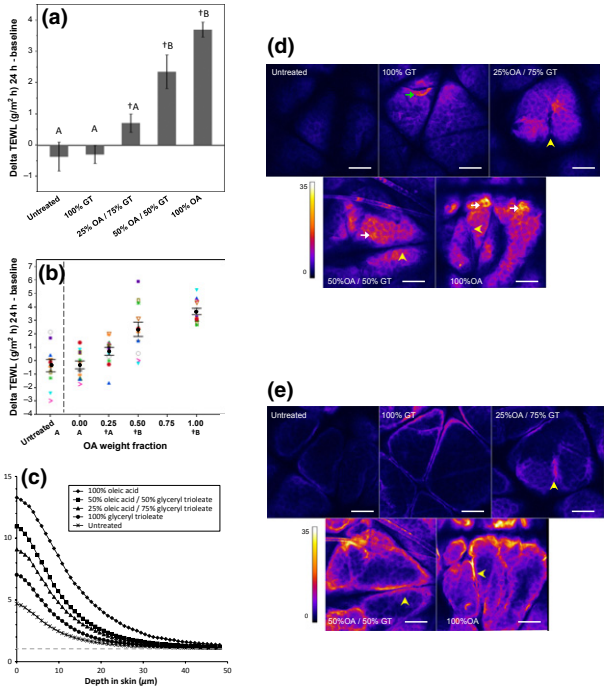

Figure 1. Application of Oleic Acid (OA), but not Glyceryl Trioleate (GT), disrupts skin barrier function. (a) Average changes in TEWL at untreated control sites and sites treated with OA, GT and their mixtures. TEWL increases over baseline values in sites treated with OA and OA/GT mixtures (†, $P < 0.05$, paired t-test), but not in untreated sites and sites treated with 100% GT. The TEWL increase in sites treated with 100% OA and 50% OA/50% GT is greater than that in sites treated with 25% OA/75% GT, 100% GT and untreated control (treatments not connected by the same letter are significantly different, one-way ANOVA with Tukey's HSD post-test, $P < 0.05$). Error bars represent 1 standard error of the mean (SEM). (b) When GT is considered to be the vehicle, a dose response in change in TEWL with increasing weight fraction of OA is observed. Within-subject trends follow trends observed in mean values (black circles represent the mean, and error bars represent 1 SEM). (c) Penetration of sodium fluorescein is measured *in vivo* through fluorescence confocal microscopy. Fluorescence intensity profile, normalized to laser power, is higher at the surface of the skin in sites treated with OA and OA/GT mixtures. Elevated fluorescence is observed throughout the stratum corneum and into the viable epidermis. Background signal is indicated by the grey dashed line. (d,e) Representative normalized fluorescence images at the surface of the SC (d) and 20 μm into the skin (e). Localized areas of elevated fluorescence are observed at the surface of the skin (white arrows) and in clumps of partially desquamated corneocytes (green arrow). Fluorescence is observed in the bottom of glyphics, but not at the surface (yellow arrowheads). Scale bars are 100 μm.

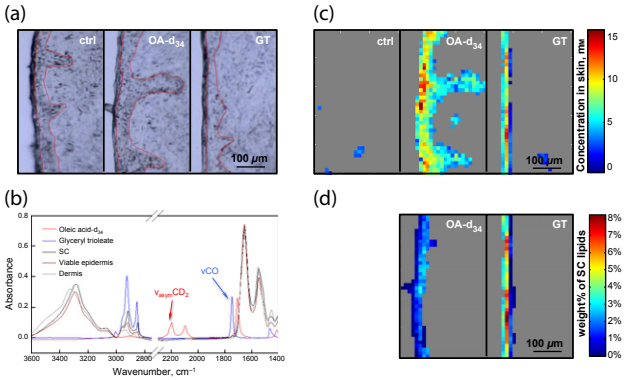

Figure 2. Detection of OA-d_{34} and GT penetration *ex vivo*. (a) Microscopic images of skin cross-sections, with the SC located to the left of each image. The untreated control sample and samples treated with OA-d_{34} and GT are placed from left to right. The SC/viable epidermis and viable epidermis/dermis boundaries are outlined with thin red lines. (b) IR spectra of pure OA-d_{34} (red), GT (blue), SC (black), viable epidermis (brown) and dermis (grey). (c) Images from the same sections shown in (a) of OA-d_{34} or GT concentration in untreated control, OA-d_{34} concentration in OA-d_{34} treated skin and GT concentration in GT treated skin, left to right, respectively. Detection limits were set with thresholds on the peak height at 2196 or 1742/cm to minimize detection in the untreated control sample, as no deuterated compounds and/or minimal amounts of esters (with sebum removed by tape stripping) were present in the untreated skin. (d) Levels of OA-d_{34} and GT in SC regions expressed as the mass percentage of endogenous SC lipids.

To assess the outside-in epidermal barrier function, the penetration of fluorescein dye into the skin after treatment was evaluated semi-quantitatively with fluorescence confocal microscopy. Average fluorescence intensity decreased with depth into skin for all treatments (Fig. 1c). Fluorescence intensity was elevated versus control in all treated sites. Profiles increased with increasing OA fraction monotonically up to 30 μm. Strong fluorescence was observed at the cell outlines, presumably representing fluorescein dye localized to the continuous lipid phase in the SC (Fig. 1d) and to the cell membranes in the viable epidermis (Fig. 1e). Partially desquamated corneocytes also appeared to strongly fluoresce (Fig. 1d, green arrow). Dye also accumulated in the glyphics, serving as a secondary source for permeation (Fig. 1d–e, yellow arrowheads).

Ex vivo skin penetration

The penetration of OA and GT was directly imaged in excised skin with IR microspectroscopy. Boundaries between the SC/viable epidermis and viable epidermis/dermis are evident in marked images of skin cross-sections (Fig. 2a). In the IR spectra of controls (Fig. 2b), the asymmetric CD_2 stretching band ($\nu_{asym}CD_2$) at ~2196/cm and the ester carbonyl stretching band (νCO) at ~1742/cm are distinct from characteristic skin bands. Intensities of these peaks were used to track the concentrations of OA-d_{34} and GT in skin, respectively (Fig. 2c–d). The control image appears mostly grey with a few pixels detected as GT, which arose from residual sebum on the skin surface and inside a hair follicle. In the treated samples, pixels with OA-d_{34} or GT levels lower than the detection limit are also shown in grey. The highest OA-d_{34} concentration was observed in the SC region. OA-d_{34} also permeated into the viable epidermis at a significant concentration but was not observed in the dermal region. In the GT treated sample, the GT signal was only observed in the first one or two columns of lateral pixels, indicating that GT slightly penetrated into the SC or that

some GT remained on the skin surface after wiping. Overall, OA penetrated deeper into skin than GT. The OA and GT levels in the SC region are also shown as a percentage of intrinsic skin lipids (Fig. 2c–d), assuming a density of 1 g/cm^3 for the skin sections and that lipids are 15% of the SC dry weight (38). It is shown that the highest OA-d_{34} level was around ~4 wt% of the endogenous SC lipids, whereas GT may be found at a relatively higher concentration (6–8%) in the top layers, or on top, of the SC. The use of acyl chain perdeuterated OA-d_{34} also allows us to study the effects of OA treatment on the acyl chain order of endogenous skin lipids. The frequencies of the methylene stretching bands are sensitive to acyl chain order; the lower the frequency, the more ordered the acyl chains (39). However, no significant differences in SC lipid ordering were observed between the OA-d_{34} treated and the control samples. This is mainly due to the large skin-to-skin variation (even among skin sections from the same donor) and the limited spatial resolution in this imaging approach (~10 μm) compared with the SC thickness (~20 μm).

Miscibility of SC lipids with OA and GT

To understand the observed differences in the resultant barrier properties, molecular interactions between OA/SC lipids and GT/SC lipids were studied with a SC lipid model composed of equimolar ceramide, cholesterol and palmitic acid in Langmuir monolayers. We defined a unit GT (uGT) as containing one oleyl chain (i.e. one-third of a GT molecule). The individual π-A isotherms for the SC lipids, OA and uGT are plotted in the inset of Fig. 3a. Compared with the densely packed solid-like SC lipid film, both OA and uGT formed expanded monolayers with the latter collapsing at a low surface pressure. The molecular areas observed per SC lipid increased with increasing amounts of OA or uGT (Fig. 3a). Before the plateau at 17–20 mN/m for the uGT containing films, a greater increase in area per SC lipid was observed with the addition of uGT compared with OA. With further compression, uGT was squeezed out of the monolayer.

Molecular interactions between SC lipids and OA or GT were evaluated by calculating the excess Gibbs energy of mixing, ΔG_{ex} (18, 31). For monolayers with multiple components that are either ideally mixed or completely phase separated, ΔG_{ex} is zero and the additional components do not contribute to film stability. ΔG_{ex} was negative for all OA mixtures at all the surface pressures studied (Fig. 3b), indicating that there are preferential interactions between OA and SC lipids compared with their intra-species interactions. The magnitude of ΔG_{ex} increased with surface pressure. In contrast, ΔG_{ex} was positive for the SC lipid/uGT mixtures, indicating that the interactions between SC lipids and uGT are more repulsive. We suggest that preferential hydrophobic acyl chain molecular interactions between OA and SC lipids are significant, contributing to the permeability of OA in skin.

Oleic acid disrupts SC lipid order *in vivo*

In Study 2, the application of OA-d_{34} *in vivo* resulted in similar TEWL increases as observed in Study 1 (data not shown). Application of perdeuterated OA permitted monitoring both the OA-d_{34} penetration and SC lipid acyl chain order independently via ATR-FTIR. Because the IR beam only penetrates 1–2 μm into skin with the ZnSe ATR substrate, spectra are result from the top SC layers, averaged over a large lateral area. ATR-FTIR is therefore better suited to study the changes in SC lipid order before and after topical treatment, compared with the IR imaging approach,

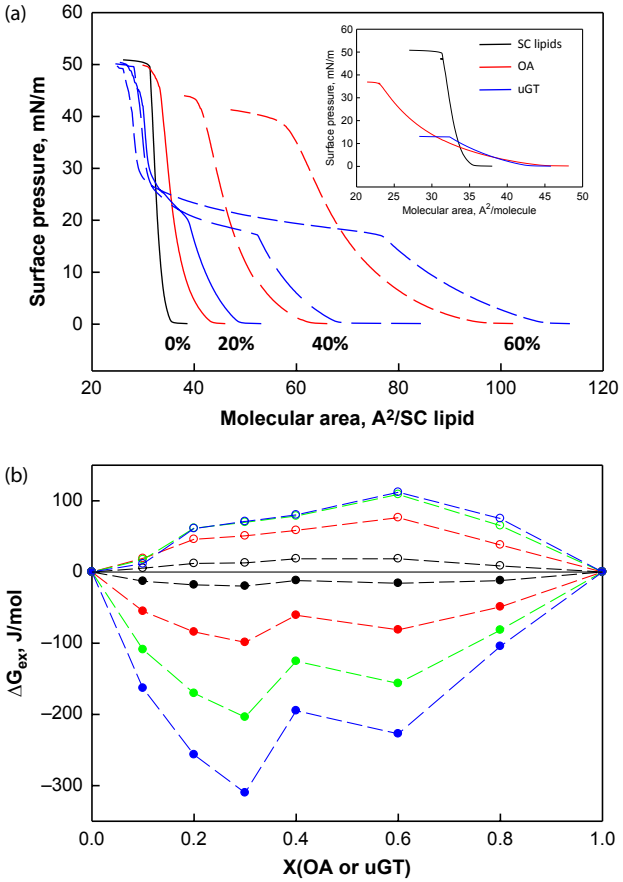

Figure 3. Interactions of OA or GT with model SC lipids in monolayers. (a) π-A isotherms of SC lipids (black), SC lipid/OA mixtures (red) and SC lipid/uGT mixtures (blue). The mole percentage of OA or uGT in the mixtures is labelled on the graph. Inset: π-A isotherms of SC lipids (black), OA (red) and uGT (blue). (b) The excess energy of mixing for SC lipid/OA mixtures (filled circles) and SC lipid/uGT mixtures (open circles) at 1 (black), 5 (red), 10 (green) and 15 (blue) mN/m as a function of monolayer composition.

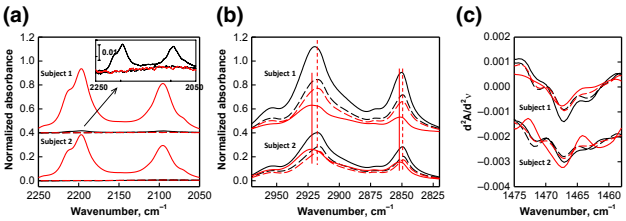

Figure 4. Effects of OA-d_{34} on the endogenous SC lipid order. ATR-FTIR spectra, normalized to the Amide I band intensity at ~1646/cm, of untreated sites (black, control) and OA-d treated sites (red) before OA-d application (dashed lines) and 24 h after application (solid lines) in (a) the CD_2 stretching region demonstrating OA-d penetration into skin, (b) CH_2 stretching region and (c) second derivative spectra of the CH_2 scissoring region. Inset in (a) enlarged spectra of the CD_2 stretching region to display the control site of subject 1, 24 h after treatment (see text, for details).

when spatial resolution is not required. Topically applied OA-d_{34} penetrated into the SC, confirmed by the presence of CD_2 stretching bands in spectra collected 24 h after application (Fig. 4a). The effects of OA-d_{34} on SC lipid order were monitored through both the CH_2 stretching band and CH_2 scissoring band (18, 31). The

24-h *in vivo* treatment of OA-d_{34} shifted the CH_2 stretching bands to higher frequencies in both subjects (Fig. 4b), indicating that OA-d_{34} disorders SC lipid acyl chains. A small amount of OA-d_{34} was detected in the control site of subject 1, (Fig. 4a, inset), which may contribute to the small frequency shift observed in the 24-h control site spectrum (Fig. 4b). This trace amount of OA-d_{34} is likely due to lateral transport from the treated site to the adjacent control site. Additional sites were measured to further investigate lateral transport, and diminishing concentrations of OA-d_{34} were observed up to 8 cm from the treatment site. In subject 2, the treated site and control site were placed on different arms to avoid this effect. OA-d_{34} also affected the acyl chain packing of SC lipids. Three peaks were observed in the second derivative spectra of the CH_2 scissoring band in both subjects before OA-d_{34} application (Fig. 4c). The centre peak at ~1467/cm arises from SC lipids that are packed in hexagonal and liquid crystalline phases, while the two shoulders at ~1463 and 1472/cm are from orthorhombic phase. After OA-d_{34} treatment, the two shoulders diminished while the centre peak broadened, indicating that the fraction of orthorhombic phase decreased. Overall, OA-d_{34} is observed to penetrate into SC *in vivo*, disordering SC lipids and shifting their packing towards less densely packed phases.

Discussion

Plant-derived oils have been traditionally used as massage oils and have recently gained popularity in skincare formulations. Several studies have investigated the effects of plant oils as skin protectants (40, 41). However, the presence of FFAs in plant oils and their associated skin penetration requires more thorough study. Herein, the effects of several OA/GT mixtures on skin barrier function were studied *in vivo*. The mixtures were found to disrupt both the inside-out (TEWL) and outside-in (fluorescein penetration) skin barrier functions in an OA dose-dependent fashion. A single topical application of the mixtures with >25% OA was able to elevate TEWL and fluorescein penetration in 24 h, suggesting that the occlusive effects of triglycerides, major component of plant oils, are not able to counteract the skin barrier disruption caused by FFAs. Further efforts should be devoted to elucidate the maximum FFA percentage in plant-oil-based formulations to guarantee safe repetitive topical application.

Despite the same acyl chain length and unsaturation level, OA and GT interact differently with SC lipids, penetrating skin to dissimilar depths. OA displayed preferential interactions with SC lipids and was able to penetrate to the dermal–epidermal junction. OA penetration was confirmed clinically, where it was observed to disorder lipid packing in the outer layers of the SC. Alternatively, the glycerol head group of GT presumably hinders the mobility and packing efficiency of GT. Mixing of GT and SC lipids was not thermodynamically preferred. GT remained on the skin surface, with minimal penetration into the SC, thus having minimal effects on skin barrier function. An earlier report predicted skin permeation based on the lipophilicity and molecular weight of permeants (42). The current combination of monolayer results and IR imaging of skin permeation suggests that the degree of mixing between OA or GT and SC lipids is indicative of the extent of SC penetration. Determination of the miscibility between permeants and SC lipids may offer an experimental method to complement empirical approaches commonly used in predicting the extent of skin permeation and warrants further study (43).

In conclusion, we have demonstrated that OA mixes with and disorders the outer layers of SC lipids and penetrates through the SC and viable epidermis. Our *ex vivo* penetration study and *in vitro* physicochemical investigation suggests that the chemical affinity between OA and skin lipids facilitates its entrance to the ordered SC lipid domains. The resultant structural disruption contributes to clinically measurable impaired barrier function. We demonstrate that higher levels of OA lead to greater disruptions of the skin barrier.

Acknowledgements

This study is funded in full by Johnson & Johnson Consumer Companies, Inc. The clinical studies were designed by MCMC and RMW and conducted by MCMC and PS. The *ex vivo* IR imaging experiments and monolayer experiments were designed by GM and RMW and were conducted by GM. All authors contributed to data analyses and interpretation. MCMC and GM prepared the manuscript, and all authors contributed to critical review of the manuscript.

Conflict of interest

MCMC, GM and RMW are employees of Johnson & Johnson Consumer Companies, Inc. PS, CRF and RM declare no conflict of interest.

References

1 Janssens M, van Smeden J, Gooris G S *et al.* J Lipid Res 2012: **53**: 2755–2766.
2 Bouwstra J A, Gooris G S, van der Spek J A *et al.* J Invest Dermatol 1991: **97**: 1005–1012.
3 Moore D J, Rerek M E, Mendelsohn R. Biochem Biophys Res Commun 1997: **231**: 797–801.
4 Damien F, Boncheva M. J Invest Dermatol 2010: **130**: 611–614.
5 Groen D, Poole D S, Gooris G S *et al.* Biochim Biophys Acta 2011: **1808**: 1529–1537.
6 Berthaud F, Boncheva M. Exp Dermatol 2011: **20**: 255–262.
7 Bouwstra J A, Ponec M. Biochim Biophys Acta 2006: **1758**: 2080–2095.
8 Lee M H, Lim B, Kim J W *et al.* Soft Matter 2012: **8**: 1539–1546.
9 Marschewski M, Hirschberg J, Omairi T *et al.* Exp Dermatol 2012: **21**: 921–925.
10 Bleck O, Abeck D, Ring J *et al.* J Invest Dermatol 1999: **113**: 894–900.
11 Janssens M, Mulder A A, van Smeden J *et al.* Biochim Biophys Acta 2013: **1828**: 1814–1821.
12 Pilgram G S, Vissers D C, van der Meulen H *et al.* J Invest Dermatol 2001: **117**: 710–717.
13 Lavrijsen A P, Bouwstra J A, Gooris G S *et al.* J Invest Dermatol 1995: **105**: 619–624.
14 Wohlrab J, Vollmann A, Wartewig S *et al.* Biopolymers 2001: **62**: 141–146.
15 Thakoersing V S, Danso M O, Mulder A *et al.* Exp Dermatol 2012: **21**: 865–870.
16 Ananthapadmanabhan K P, Mukherjee S, Chandar P. Int J Cosmet Sci 2013: **35**: 337–345.
17 Denda M, Koyama J, Namba R *et al.* Arch Dermatol Res 1994: **286**: 41–46.
18 Saad P, Flach C R, Walters R M *et al.* Int J Cosmet Sci 2012: **34**: 36–43.
19 Benfeldt E, Serup J, Menne T. Br J Dermatol 1999: **140**: 739–748.
20 Coderch L, de Pera M, Perez-Cullell N *et al.* Skin Pharmacol Appl Skin Physiol 1999: **12**: 235–246.
21 Rodriguez G, Cocera M, Rubio L *et al.* Phys Chem Chem Phys 2012: **14**: 14523–14533.
22 Barbosa-Barros L, Barba C, Rodriguez G *et al.* Mol Pharm 2009: **6**: 1237–1245.
23 Tanojo H, Boelsma E, Junginger H E *et al.* Skin Pharmacol Appl Skin Physiol 1998: **11**: 87–97.
24 Katsuta Y, Iida T, Inomata S *et al.* J Invest Dermatol 2005: **124**: 1008–1013.
25 Francoeur M L, Golden G M, Potts R O. Pharm Res 1990: **7**: 621–627.
26 Tanojo H, Bos-van Geest A, Bouwstra J A *et al.* Thermochim Acta 1997: **293**: 77–85.
27 Naik A, Pechtold L A R M, Potts R O *et al.* J Controlled Release 1995: **37**: 299–306.
28 Ongpipattanakul B, Burnette R R, Potts R O *et al.* Pharm Res 1991: **8**: 350–354.
29 Rowat A C, Kitson N, Thewalt J L. Int J Pharm 2006: **307**: 225–231.
30 Hoopes M I, Noro M G, Longo M L *et al.* J Phys Chem B 2011: **115**: 3164–3171.
31 Mao G, Vanwyck D, Xiao X *et al.* Langmuir 2013: **29**: 4857–4865.
32 Diraman H, Dibeklioglu H. J Am Oil Chem Soc 2009: **86**: 663–674.
33 Mailer R. J Am Oil Chem Soc 2004: **81**: 823–827.

34 Patzelt A, Lademann J, Richter H *et al.* Skin Res Technol 2012: **18**: 364–369.
35 Nanayakkara G R, Bartlett A, Forbes B *et al.* Int J Pharm 2005: **301**: 129–139.
36 Takeuchi Y, Yamaoka Y, Fukushima S *et al.* Biol Pharm Bull 1998: **21**: 484–491.
37 Mao G, Flach C R, Mendelsohn R *et al.* Pharm Res 2012: **29**: 2189–2201.
38 Wertz P W, van den Bergh B. The physical, chemical and functional properties of lipids in the skin and other biological barriers. Chem Phys Lipids 1998: **91**: 85–96.
39 Mendelsohn R, Flach C R, Moore D J. Biochim Biophys Acta 2006: **1758**: 923–933.
40 Danby S G, AlEnezi T, Sultan A *et al.* Pediatr Dermatol 2013: **30**: 42–50.
41 Viola P, Viola M. Clin Dermatol 2009: **27**: 159–165.
42 Potts R O, Guy R H. Pharm Res 1992: **9**: 663–669.
43 Mitragotri S, Anissimov Y G, Bunge A L *et al.* Int J Pharm 2011: **418**: 115–129.